Ann. Geophys., 30, 1567–1573, 2012
www.ann-geophys.net/30/1567/2012/
doi:10.5194/angeo-30-1567-2012

Annales Geophysicae

Anisotropic pitch angle distribution of ∼100 keV microburst electrons in the loss cone: measurements from STSAT-1

J. J. Lee[1], G. K. Parks[2], E. Lee[3], B. T. Tsurutani[4], J. Hwang[1], K. S. Cho[1], K.-H. Kim[3], Y. D. Park[1], K. W. Min[5], and M. P. McCarthy[6]

[1]Department of Space Science Research, Astronomy and Space Science Institute, Daejeon, Korea
[2]Space Sciences Laboratory, University of California, CA, USA
[3]School of Space Research, Kyung Hee University, Gyeonggi, Korea
[4]Jet Propulsion Laboratory, California Institute of Technology, Pasadena, CA, USA
[5]Department of Physics, Korea Advanced Institute of Science and Technology, Daejeon, Korea
[6]Department of Planetary and Space Sciences, University of Washington, Seattle, WA, USA

Correspondence to: J. J. Lee (jjlee@kasi.re.kr)

Received: 27 December 2011 – Revised: 17 September 2012 – Accepted: 10 October 2012 – Published: 6 November 2012

Abstract. Electron microburst energy spectra in the range of 170 keV to 360 keV have been measured using two solid-state detectors onboard the low-altitude (680 km), polar-orbiting Korean STSAT-1 (Science and Technology SATellite-1). Applying a unique capability of the spacecraft attitude control system, microburst energy spectra have been accurately resolved into two components: perpendicular to and parallel to the geomagnetic field direction. The former measures trapped electrons and the latter those electrons with pitch angles in the loss cone and precipitating into atmosphere. It is found that the perpendicular component energy spectra are harder than the parallel component and the loss cone is not completely filled by the electrons in the energy range of 170 keV to 360 keV. These results have been modeled assuming a wave-particle cyclotron resonance mechanism, where higher energy electrons travelling within a magnetic flux tube interact with whistler mode waves at higher latitudes (lower altitudes). Our results suggest that because higher energy (relativistic) microbursts do not fill the loss cone completely, only a small portion of electrons is able to reach low altitude (∼100 km) atmosphere. Thus assuming that low energy microbursts and relativistic microbursts are created by cyclotron resonance with chorus elements (but at different locations), the low energy portion of the microburst spectrum will dominate at low altitudes. This explains why relativistic microbursts have not been observed by balloon experiments, which typically float at altitudes of ∼30 km and measure only X-ray flux produced by collisions between neutral atmospheric particles and precipitating electrons.

Keywords. Magnetospheric physics (Energetic particles, precipitating)

1 Introduction

Microbursts represent electron precipitation having durations of less than ∼1 s at $L = 4$–8 (Parks et al., 1965; Parks, 1978; O'Brien et al., 2003). Microburst precipitation has been observed since the early sixties by balloon-borne X-ray experiments in the energy range of ∼20–100 keV (Anderson and Milton, 1964). Microbursts can be characterized by exponential energy spectra with e-folding energies $E_0 \sim 5$–20 keV (Anderson et al., 1966; Lampton, 1967; Rosenberg et al., 1990; Reinard et al., 1997; Datta et al., 1997). To distinguish them from the relativistic microbursts, we call these low energy microbursts.

Cyclotron resonance between electrons and chorus has been suggested as a possible mechanism for low energy microbursts (Rosenberg et al., 1990; Skoug et al., 1996; Tsurutani et al., 2009; Lakhina et al., 2010). Chorus is a bursty whistler mode wave with elements of ∼0.1–1 s and has similar time scales as electron microbursts (Tsurutani and Smith, 1974). Moreover, the coincident occurrences between microburst and VLF chorus waves have given support to the idea that low energy microbursts are produced by

wave-electron cyclotron resonance interactions (Rosenberg et al., 1981).

On the other hand, Imhof et al. (1992) and Nakamura et al. (2000) reported observations of impulsive electron precipitation with energies >1 MeV on polar orbiting spacecraft and called them relativistic microbursts (Blake et al., 1996; O'Brien et al., 2004). It is known that relativistic microbursts are associated with large amplitude whistler mode waves (Johnston and Anderson, 2010; Kersten et al., 2011). However, relativistic microbursts have not been observed by balloon-borne experiments to date (Millan et al., 2002). Furthermore it is not known at this time how the two "types" of microbursts are related or if they are related at all.

Lee et al. (2005) reported the energy spectra of electron microbursts observed by STSAT-1 in the range of 170 keV to 360 keV, which represent the intermediate energy range between relativistic and low energy microbursts. This preliminary report showed there was no time delay between the appearance of trapped (perpendicular) and precipitated (parallel) microbursts, indicating microbursts were generated by prompt loss cone filling within a time scale of ∼50 ms (the time resolution of the instruments) or less. They also reported the e-folding energies of microbursts increase during storm time and the perpendicular component energy spectra are harder than the parallel component. However, particular details on the latter were not given.

In the current study, the STSAT-1 energetic electron data is further analyzed to determine the anisotropy of the microburst energy spectra. We also discuss the implications for microburst anisotropic precipitation.

2 Observation

To measure precipitating electrons, two SSTs (solid state telescope) on STSAT-1 were launched into a sun-synchronous, low-altitude (680 km) orbit on 27 September 2003. STSAT-1's 3-axis attitude control system aligned one SST to the Earth's magnetic field direction to measure precipitated electrons and the other perpendicular to the magnetic field to measure quasi-trapped electrons (Lee et al., 2010). This configuration has allowed us to study precipitation from quasi-trapped electrons in the energy range ∼190 keV to 360 keV (perpendicular) and ∼170 keV to 330 keV (parallel) with 30 energy channels. The SSTs measured electrons with 50 ms time resolution, adequate to resolve microburst structures (Lee et al., 2005). Each SST had a 33.9° field of view (FOV) with a geometric factor of 0.045 cm^2 sr. An aluminum coated Lexan foil was placed in front of each detector to shield against ions and solar UV.

STSAT-1 was operated successfully for approximately 300 passes through the auroral zone and lasted until 31 March 2005. During this period, electron microbursts were detected on six different occasions. Figure 1 shows an example of microburst precipitation detected on 10 November 2004 during the recovery phase of a strong magnetic storm that started on 8 November 2004 (Tsurutani et al., 2008). This storm reached a minimum Dst index of −373 nT. During this magnetic storm, strong substorm particle injections were observed at geostationary orbit (not shown). The AE index was ∼625 nT and the magnetic local time was ∼07:00-08:00 MLT (morning sector) at the time the electron microbursts were detected. This local time is the general time when microbursts are most commonly detected (O'Brien et al., 2003) and also when chorus is most common (Tsurutani and Smith, 1977).

The differential electron fluxes plotted (spectrogram format) for the perpendicular- and parallel-pointing SSTs (top two panels) show impulsive bursts during the 60-s interval. Thirty-five microbursts were detected with durations varying between ∼150 ms and 1.2 s. The perpendicular (top panel) SST detected quasi-trapped electrons mirroring at the satellite altitude. The parallel electron spectrogram (panel 2) shows that the atmospheric loss cone, ∼60° at 680 km altitude, was nearly empty (below the instrument threshold) except for the short duration when the impulsive precipitation was observed. Because the durations of the microbursts are significantly shorter than the bounce period of electrons, bouncing echoes could be expected such as isolated bursts observed by SAMPEX mission (Blake et al., 1996). However, in Fig. 1, no such bouncing echoes were observed. If there were bouncing echoes, microburst electrons should not have been detected by the parallel detector because the detector can measure only electrons having pitch angles in the range of 0–17°. Particles within the loss cone will collide with upper atmospheric atoms and molecules and will be lost. Thus two detectors, parallel and perpendicular clearly show the microbursts observed by STSAT-1 are precipitating electrons without contamination of bouncing echoes.

The microburst energy spectra are fitted by an exponential form, $dJ/dE = Ae^{(-E/E_0)}$, where dJ/dE is the differential flux, E is the electron energy, and E_0 is the e-folding energy. The third panel from the top shows the e-folding energies for the perpendicular component electrons in black and parallel electrons in blue throughout the time interval that microbursts were detected. It can be noted that the perpendicular microburst e-folding energies are nearly identical to the background e-folding energies. This means there is no significant energy gain or loss occurring during electron microbursts. In addition, it should be noted that the parallel e-folding energies are slightly, but consistently smaller than the perpendicular e-folding energies (in microburst precipitation).

In this paper, a key observation is that perpendicular microburst fluxes are higher than the parallel ones, as shown in panel 4 in which the total electron fluxes summed in the detector's common energy range of 190 keV–330 keV. This indicates microbursts have anisotropic pitch angle distributions and the loss cone is not filled completely. The microburst electron fluxes parallel to B decrease faster than the

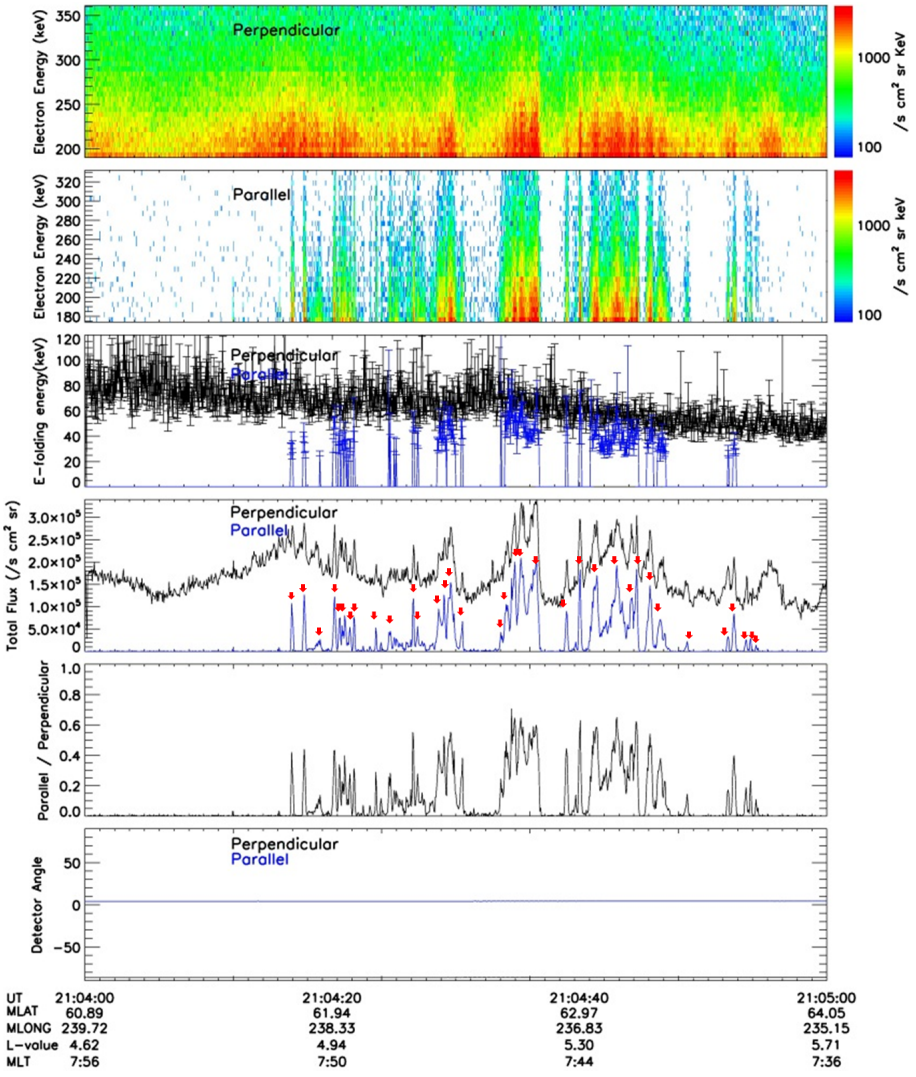

Fig. 1. Electron microbursts observed during the recovery phase of a magnetic storm on 10 November 2004. The panels from top to bottom are: perpendicular to B (panel 1), parallel to B (panel 2) electron spectrograms, e-folding energies of perpendicular (black) electrons and parallel (blue) electrons (panel 3), total fluxes which is the sum of differential fluxes from 190 keV to 330 keV, common energy range of parallel and perpendicular detectors (panel 4), the total flux ratio of parallel to perpendicular flux (panel 5) and detector view direction relative to the geomagnetic field (bottom). In panel 4, the red arrows indicate each burst.

perpendicular fluxes with increasing energy (see e-folding energies in panel 3). This observation suggests that the pitch angle anisotropy increases for the higher energy electrons. Our observation is consistent with the results obtained by Lampton (1967) who observed anisotropic pitch angle distributions with rocket experiments. In the following section, we focus on how such microburst anisotropy occurs and how it is related with acceleration/loss processes of radiation belt electrons. The bottom panel in Fig. 1 shows the angle between the detectors and the geomagnetic field. The parallel SST was aligned along the magnetic field to within 5°.

3 Microburst energy spectra

Figure 2 shows the average energy spectra of electron microbursts measured by STSAT-1 for storm and quiet-moderate times. Points in red represent storm time ($-300\,\text{nT} < \text{Dst} < -100\,\text{nT}$) data and blue gives quiet-moderate time ($-100\,\text{nT} < \text{Dst} < 0\,\text{nT}$) data. While 45 microbursts were observed during storm time recovery phase, 22 were observed during quiet-moderate time for 4 orbits in 2004. The asterisks denote the parallel component energy spectra and diamonds the perpendicular component energy spectra (for individual microburst energy spectra, see Fig. 3 in Lee et al., 2005). Figure 2 shows both parallel and perpendicular e-folding energies increased in storm

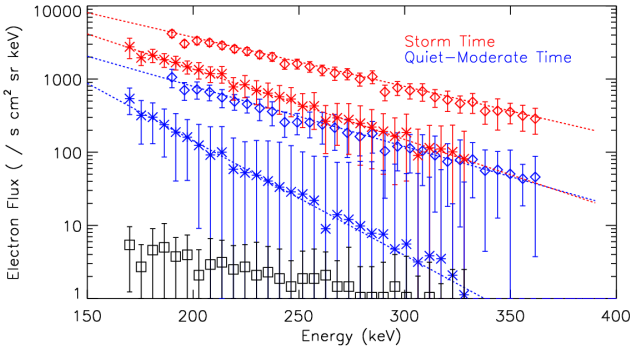

Fig. 2. Average electron energy spectra for perpendicular to B (diamond) and parallel to B (asterisk) pitch angle components. Blue and red colors refer to quiet-moderate and storm time data. Black square symbols represent background of the parallel detector.

time, from 52.8 ± 2.0 keV to 64.6 ± 2.3 keV in the perpendicular pitch angle direction, and from 27.7 ± 1.0 keV to 45.1 ± 1.4 keV in parallel pitch angle direction. The black square symbols indicate the background counting of the parallel detector. The parallel component error bars represent the standard deviation of microburst counting flux. This is not small for quiet-moderate times. It should be noted that the average 170 keV microburst flux is significantly (two orders of magnitude) larger than background noise. Therefore, the parallel microburst e-folding energy of ∼45 keV (see the slopes of energy spectra) during the storm is significantly larger than quiet-moderate time values (∼27 keV). Considering chorus wave activity increases during storms, it seems possible that large amplitude waves might generate higher e-folding energy microbursts. Another possible explanation is that storm time convection electric fields convect the plasmasheet plasma deeper into the magnetosphere, energizing electrons by betatron acceleration (Gonzalez et al., 1994). In addition, it should be noted that the parallel e-folding energy and fluxes are smaller than the perpendicular ones even during the storm. While Lorentzen et al. (2001) and O'Brien et al. (2004) calculated microburst loss rate by assuming isotropic pitch angle distributions, our observations indicate energetic electron loss might be smaller than their estimation.

4 Resonance condition for wave particle interaction

We interpret our observations using the cyclotron resonance wave-particle theory. The specific question we will examine is how electron microbursts can be produced with different parallel and perpendicular e-folding energies. The wave particle interaction mechanism requires a resonance condition satisfying

$$\omega - k_{\parallel} v_{\parallel} = n \frac{\Omega_c}{\gamma}, \tag{1}$$

where ω is the wave frequency in rad s^{-1}, $k_{\parallel}$ and $v_{\parallel}$ are the parallel components of the wave vector and particle velocity with respect to the ambient magnetic field $\boldsymbol{B}$, Ω_c is the electron cyclotron frequency, γ is the relativistic factor and n is an integer denoting the cyclotron harmonic number. To model STSAT-1 observations, we assume different energy (10 keV, 100 keV, 1 MeV and 10 MeV) electrons interacting with 1 kHz whistler mode waves propagating along magnetic field, with the cyclotron frequency ∼15.1 kHz in a background magnetic field of ∼542 nT (the plasma frequency is 260 kHz) at the equator. The electrons and waves are moving in opposite directions to satisfy the Doppler-shifted resonance condition.

In Eq. (1), the gyro-frequency, Ω_c is a function of the magnetic field. The wave vector $\boldsymbol{k}$ can be expressed as a function of ω from the dispersion relation Eq. (2) where ω_p is the plasma frequency, which in turn depends on the thermal plasma density. If we assume the plasma content of a magnetic flux tube is constant along the field, then the plasma density depends linearly on the magnetic field and ω_p also becomes a function of the magnetic field as shown in Eq. (3) where n_p is the thermal plasma density. Now, the resonance condition can be expressed as a function of the magnetic field, and we can solve Eq. (1) for the magnetic latitude for fixed energy electrons in a dipole field.

The above assumption that the plasma density depends linearly on the background geomagnetic field might not be correct. However, we make this rough approximation to obtain general results. Note that whistler mode waves propagate through a magnetic flux tube, and the plasma density can be expressed in terms of the magnetic latitude, high densities at high latitudes and low densities at low latitudes. In reality, the solution of Eq. (1) might be different from our results, however the overall trends are the important factors here.

$$\frac{K^2 c^2}{\omega^2} = 1 + \frac{\omega_p^2}{\omega(\Omega_c - \omega)} \tag{2}$$

$$\frac{\omega_p}{2\pi} = 8.98\sqrt{n_p} \propto \sqrt{B_0} \tag{3}$$

Figure 3 shows a plot of $\omega - k_{\parallel} v_{\parallel} - n\frac{\Omega_c}{\gamma}$ as a function of the magnetic latitude when 1 kHz whistler mode waves are applied to 10 keV, 100 keV, 1 MeV and 10 MeV electrons for $n = 1$ (solid lines) and $n = 2$ (dotted lines). Here, we assumed a plasma density of 2/cm^3 at the equatorial region (Carpenter and Anderson, 1992) and L is 5.5. When $\omega - k_{\parallel} v_{\parallel} - n\frac{\Omega_c}{\gamma} = 0$, a resonance condition is satisfied and wave-particle interactions alter the electron's pitch angle (Tsurutani and Lakhina, 1997). As shown in Fig. 3, 10 keV electrons do not have a solution satisfying the resonance condition, so their pitch angles are not changed by the wave-particle interaction. On the other hand, 100 keV electrons interact with waves for $n = 1$ in the equatorial region where the loss cone angle is small and electrons can be scattered to fill

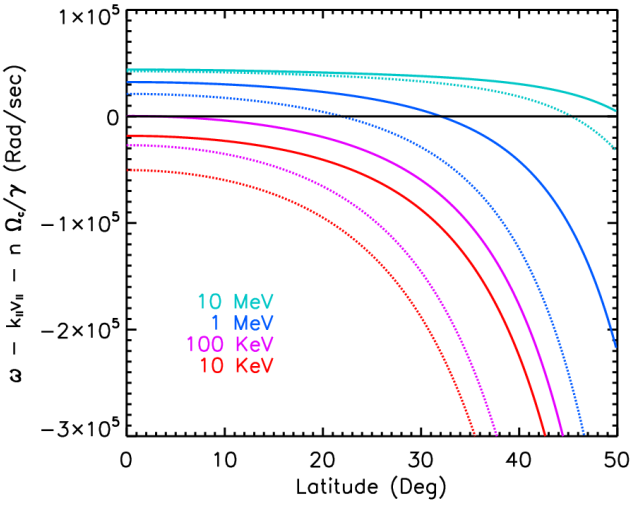

Fig. 3. Resonance condition as a function of the magnetic latitude for 1 kHz waves interacting with 10 keV, 100 keV, 1 MeV and 10 MeV electrons. The solid and dotted lines show the first and second order resonance conditions, respectively. The horizontal solid black line represents the satisfying of the Doppler-shifted resonance condition.

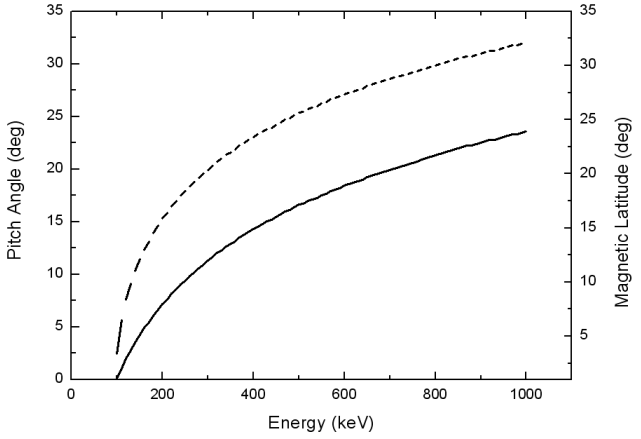

Fig. 4. Magnetic latitudes where the resonance condition of Eq. (1) is satisfied for different electron energies (dashed line). The unfilled pitch angles of microbursts that are expected to be measured at 680 km altitude (solid line).

the loss cone. MeV electrons can interact with waves at high latitudes (low altitude) where the loss cone angle is larger than at the equator. In this case, high energy electrons have to travel through a larger angle in velocity space to reach a pitch-angle of zero degrees during interaction with waves. It is thus more difficult for high energy electrons to be scattered into the loss cone and contribute to the microburst precipitation.

In Fig. 3, the higher order of cyclotron harmonic can move the interaction region to lower latitudes and potentially produce intense field-aligned microbursts even in the high energy region. However, the wave-particle interaction mechanism is most efficient in the first-order resonance condition, and the higher order resonances are not expected to contribute significantly to the pitch angle scattering (Thorne et al., 2005).

In our simple model, we applied 1 kHz whistler mode waves. These waves satisfied the resonance condition with 0.1, 1.0, 10 MeV electrons at 3.3°, 32.1°, 50.8° magnetic latitudes, respectively. In Eq. (1), it should be noted that the lower frequency waves interact with the higher energy (higher $v_{\|}$) electrons with the same condition. For example, 500 Hz waves interact with 0.25, 1.0, 10 MeV electrons at 4.1°, 26.3°, 47.8° respectively. Thus high energy electrons interact with low frequency waves at low latitudes where the loss cone is small and potentially produces high energy microbursts. Here, it should be emphasized that in any case, fixed frequency waves interact with low energy electrons at low latitudes and high energy electrons at high latitudes. This is the key point to explain microburst energy spectral anisotropy dependence on energy.

We have considered resonance interaction between cyclotron waves and electrons and have shown that low energy microbursts can be generated at low latitudes while high energy electrons can interact with waves at high latitudes. Because the loss cone is larger at high latitudes, it might be harder to fill the loss cone by wave interactions. This prediction is consistent with our observations. Note in Fig. 2 the pitch angle range of 0°–17° (half of detector's view angle) in loss cone was filled almost 40 % for low energy (∼190 keV) microbursts while it was filled just 16 % for high energy (∼330 keV) microbursts.

5 Discussion and conclusion

In the previous section, we have shown that the unfilled loss cone angle of microbursts depends on energy. Thus, how are large pitch angles of relativistic electrons filled by wave-particle interaction? We estimate it with a simple model. Near the equator, the atmospheric loss cone angle is about 3°. This means electrons need to scatter only 3° to fill the loss cone. The factors that can affect the magnitude of pitch-angle diffusion rate include wave amplitude, interaction time and background magnetic field, depending on latitude. Since we don't have enough information on these factors, we will assume for simplicity that the pitch-angle scattering rate is 3° for one-time wave interaction and constant over the region from the equator to 30° magnetic latitude where 100–1000 keV electrons resonate with waves (Fig. 4, dashed line). So, in our simple model, 100 keV microbursts fill the loss cone completely while higher energy microbursts only partially fill the loss cone. Thus we have derived the empty loss cone angles of different energy microbursts at the altitude of 680 km as shown by the solid line in Fig. 4. Note the unfilled pitch angles, 6.3° and 11.4° at 190 keV and 330 keV,

respectively. This corresponds to filling the pitch angle in the instrument range (0°–17°) by 86 % and 55 %, respectively, when scaling the filling factor simply by the solid angle. In Fig. 2, the measurements show that only a fraction of the pitch angle range measured by the parallel detector is filled (i.e. 40 % and 16 % at 190 keV and 330 keV, respectively). The model seems to indicate microburst electron flux about two times larger than measurements in the instrument field of view. However, assuming 70 % instead of 100 % filling of instrument range at 100 keV, such as we have assumed previously, the model shows 44 % and 0 % filling at 190 keV and 330 keV, respectively. While we do not have detailed information on 100 keV microburst pitch angle distribution, the simple model qualitatively explains the observational differences between perpendicular and parallel microburst energy spectra shown in Fig. 2.

The assumption that the scattering angle rate is constant over all energy electrons might be an oversimplification. Higher energy electrons move fast and the interaction time might be shorter. In addition, high energy electrons are scattered less in pitch angle by wave interaction at high latitudes where the background magnetic field is stronger. An alternative explanation for the low flux of the 360 keV microburst electrons in comparison to low energy (∼100 keV) microburst electrons is due to decreasing chorus coherency away from the equatorial generation region (Tsurutani et al., 2011). The coherent waves can scatter electron's pitch angle more efficiently (Lakhina et al., 2010). Therefore, the scattering rate might be smaller for high energy electrons.

The anisotropic pitch angle distribution shown in Fig. 4 might explain why only low energy microbursts have been observed by balloon-borne experiments and relativistic microbursts by only space-born experiments. If relativistic microbursts have the same origin as ∼100 keV microbursts and the energy spectra can be extended to 1 MeV, the unfilled pitch angle of relativistic microbursts is about 25°, in which small numbers of electrons precipitate into the atmosphere by microburst events. Electrons scattered into atmospheric loss cone can reach low altitudes and produce X-rays detected by instruments aboard balloons at altitudes of 30 km. Our result implies only a small number of relativistic (high energy) microburst electrons can reach the dense atmosphere and produce just weak X-ray flux. Thus, the pitch-angle distribution information is crucial to identify if the relativistic microbursts and the low energy microbursts have the same source.

Since the microburst events were observed, the pitch angle anisotropy has not been studied extensively. The anisotropic pitch angle distribution of microburst should also be considered important in studying loss and acceleration processes of radiation belt electrons. It has been widely accepted that the chorus waves play a significant role in the acceleration process of electrons during geomagnetic storms (Katoh and Omura, 2007; Summers and Omura, 2007; Friedel et al., 2002). Our results show that low energy electrons are removed more efficiently by microbursts than high energy electrons. Thus the e-folding energy of trapped electrons increases, making it as if the radiation belt electrons are accelerated. This effect should be distinguished from acceleration of microburst electrons by wave-particle interaction.

Some researchers have calculated electron precipitation rates of relativistic microbursts and showed wave particle interaction is a dominant electron loss process of radiation belt-relativistic electrons (Lorentzen et al., 2001; O'Brien et al., 2004; Thorne et al., 2005). They estimated the electron loss rate using SAMPEX data assuming downward isotropic pitch angle distribution. However, based on our observations, their estimates probably represent upper limit values.

Our discussion has been on the basis of measurements obtained by two detectors, while it should be noted that the experiment does not cover a large part of loss cone (∼17°–60°). In addition, our estimate of the unfilled pitch angle range, 25° for 1 MeV electrons in Fig. 4, is not small and can be measured by a sophisticated instrument designed to resolve the electron pitch angle distributions over a wide energy range. Future missions with instruments covering a wider energy and pitch angle range will be needed to reveal the relation between low energy and relativistic microbursts.

Acknowledgements. This research has been mainly supported by the "Development of Korean Space Weather Center" project of KASI, and the KASI basic research fund. Portions of this research were performed at the Jet Propulsion Laboratory, California Institute of Technology under contract with NASA. Work of K.-H. Kim was supported by WCU program through NRF funded by MEST of Korea (R31-10016).

Topical Editor R. Nakamura thanks three anonymous referees for their help in evaluating this paper.

References

Anderson, K. A. and Milton, D. W.: Balloon observations of x-rays in the auroral zone, J. Geophys. Res., 69, 4457–4479, 1964.

Anderson, K. A., Chase, L. M., Hudson, H. S., Lampton, M., Milton, D. W., and Parks, G. K.: Balloon and rocket observations of auroral-zone microburst, J. Geophys. Res., 71, 4617–4589, 1966.

Blake, J. B., Looper, M. D., Baker, D. N., Nakamura, R., Klecker, B., and Hovestadt, D.: New high temporal and spatial resolution measurements by SAMPEX of the precipitation of relativistic electrons, Adv. Space Res., 18, 171–186, 1996.

Carpenter, D. L. and Anderson, R. R.: An ISEE/Whistler Model of Equatorial Electron Density in the Magnetosphere, J. Geophys. Res., 97, 1097–1108, 1992.

Datta, S., Skoug, R. M., McCarthy, M. P., and Parks, G. K.: Modeling of microburst electron precipitation using pitch angle diffusion theory, J. Geophys. Res., 102, 17325–17334, 1997.

Friedel, R. H. W., Reeves, G. D., and Obara, T.: Relativistic electron dynamics in the inner magnetosphere – A review, J. Atmos. Solar Terr. Phys., 64, 265–282, 2002.

Gonzalez, W. D., Joselyn, J. A., Kamide, Y., Kroehl, H. W., Rostoker, G., Tsurutani, B. T., and Vasyliunas, V. M.: What is a geomagnetic storm?, J. Geophys. Res., 99, 5771–5792, 1994.

Imhof, W. L., Voss, H. D., Mobilia, J., Datlowe, D. W., Gaines, E. E., McGlennon, J. P., and Inan, U. S.: Relativistic electron microbursts, J. Geophys. Res., 97, 13829–13837, 1992.

Johnston, W. R. and Anderson, P. C.: Storm time occurrence of relativistic electron microbursts in relation to the plasmapause, J. Geophys. Res., 115, A02205, doi:10.1029/2009JA014328, 2010.

Katoh, Y. and Omura, Y.: Relativistic particle acceleration in the process of whistler-mode chorus wave generation, Geophys. Res. Lett., 34, L13102, doi:10.1029/2007GL029758, 2007.

Kersten, K., Cattell, C. A., Breneman, A., Goetz, K., Kellogg, P. J., Wygant, J. R., Wilson III, L. B., Blake, J. B., Looper, M. D., and Roth, I.: Observation of relativistic electron microbursts in conjunction with intense radiation belt whistler-mode waves, Geophys. Res. Lett., 38, L08107, doi:10.1029/2011GL046810, 2011.

Lakhina, G. S., Tsurutani, B. T., Verkhoglyadova, O. P., and Pickett, J. S.: Pitch angle transport of electrons due to cyclotron interactions with the coherent chorus subelements, J. Geophys. Res., 115, A00F15, doi:10.1029/2009JA014885, 2010.

Lampton, M.: Daytime Observations of Energetic Auroral-Zone Electrons, J. Geophys. Res., 72, 5817–5823, 1967.

Lee, C. N., Min, K. W., Lee, J.-J., Parks, G. K., Fillingim, M. O., Lummerzheim, D., Cho, K. S., Kim, K.-H., Kim, Y. H., Park, Y. D., Han, W., Edelstain, J., and Korpela, E.: Spectral observations of FUV auroral arcs and comparison with inverted-V precipitating electrons, J. Geophys. Res., 115, A09223, doi:10.1029/2009JA015071, 2010.

Lee, J.-J., Parks, G. K., Min, K. W., Kim, H. J., Park, J., Hwang, J., McCarthy, M. P., Lee, E., Ryu, K. S., Lim, J. T., Sim, E. S., Lee, H. W., Kang, K. I., and Park, H. Y.: Energy spectra of ∼170–360 keV electron microbursts measured by the Korean STSAT-1, Geophys. Res. Lett., 32, L13106, doi:10.1029/2005GL022996, 2005.

Lorentzen, K. R., Blake, J. B., Inan, U. S., and Bortnik, J.: Observations of relativistic electron microbursts in association with vlf chorus, J. Geophys. Res., 106, 6017–6027, 2001.

Millan, R. M., Lin, R. P., Smith, D. M., Lorentzen, K. R., and McCarthy, M. P.: X-ray observations of MeV electron precipitation with a balloon-borne germanium spectrometer, Geophys. Res. Lett., 29, 2194–2197, 2002.

Nakamura, R., Isowa, M., Kamide, Y., Baker, D. N., Blake, J. B., and Looper, M.: Observations of relativistic electron microbursts in association with vlf chorus, J. Geophys. Res., 105, 15875–15885, 2000.

O'Brien, T. P., Lorentzen, K. R., Mann, I. R., Meredith, N. P., Blake, J. B., Fennell, J. F., Looper, M. D., Milling, D. K., and Anderson, R. R.: Energization of relativistic electrons in the presence of ULF power and MeV microbursts: Evidence for dual ULF and VLF acceleration, J. Geophys. Res., 108, 1329, doi:10.1029/2002JA009784, 2003.

O'Brien, T. P., Looper, M. D., and Blake, J. B.: Quantification of relativistic electron microburst losses during the GEM storms, Geophys. Res. Lett., 31, L04802, doi:10.1029/2003GL018621, 2004.

Parks, G. K.: Microburst precipitation phenomena, J. Geomag. Geoelectr., 30, 327–341, 1978.

Parks, G. K., Hudson, H. S., Milton, D. W., and Anderson, K. A.: Spatial Asymmetry and Periodic Time Variations of X-Ray Microbursts in the Auroral Zone, J. Geophys. Res., 70, 4976–4978, 1965.

Reinard, A. A., Skoug, R. M., Datta, S., and Parks, G. K.: Energy spectral characteristics of auroral electron microburst precipitation, Geophys. Res. Lett., 24, 611–614, 1997.

Rosenberg, T. J., Siren, J. C., Matthews, D. L., Marthinsen, K., Holtet, J. A., Egeland, A., Carpenter, D. L., and Helliwell, R. A.: Conjugacy of electron microbursts and vlf chorus, J. Geophys. Res., 86, 5819–5832, 1981.

Rosenberg, T. J., Wei, R., and Detrick, D. L.: Observations and modeling of wave-induced microburst electron precipitation, J. Geophys. Res., 95, 6467–6475, 1990.

Skoug, R. M., Datta, S., McCarthy, M. P., and Parks, G. K.: A cyclotron resonance model of VLF chorus emissions detected during electron microburst precipitation, J. Geophys. Res., 101, 21481–21492, 1996.

Summers, D. and Omura, Y.: Ultra-relativistic acceleration of electrons in planetary magnetospheres, Geophys. Res. Lett., 34, L24205, doi:10.1029/2007GL032226, 2007.

Thorne, R. M., O'Brien, T. P., Shprits, Y. Y., Summers, D., and Horne, R. B.: Timescale for MeV electron microburst loss during geomagnetic storms, J. Geophys. Res., 110, A09202, doi:10.1029/2004JA010882, 2005.

Tsurutani, B. T. and Lakhina, G. S.: Some basic concepts of wave-particle interactions in collisionless plasmas, Rev. Geophys., 35, 491–502, 1997.

Tsurutani, B. and Smith, E.: Postmidnight Chorus: A Substorm Phenomenon, J. Geophys. Res., 79, 118–127, 1974.

Tsurutani, B. T. and Smith, E. J.: Two types of magnetospheric ELF chorus and their substorm dependences, J. Geophys. Res., 82, 5112–5128, 1977.

Tsurutani, B., Echer, E., Guarnieri, F. L., and Kozyra, J. U.: CAWSES November 7–8, 2004, superstorm: Complex solar and interplanetary features in the post-solar maximum phase, Geophys. Res. Lett., 35, L06S05, doi:10.1029/2007GL031473, 2008.

Tsurutani, B. T., Verkhoglyadova, O. P., Lakhina, G. S., and Yagitani, S.: Properties of dayside outer zone chorus during HILDCAA events: Loss of energetic electrons, J. Geophys. Res. (Space Physics), 114, 3207, doi:10.1029/2008JA013353, 2009.

Tsurutani, B. T., Falkowski, B. J., Verkhoglyadova, O. P., Pickett, J. S., Santolik, O., and Lakhina, G. S.: Quasi-coherent chorus properties: 1. Implications for wave-particle interactions, J. Geophys. Res., 116, A09210, doi:10.1029/2010JA016237, 2011.